Colloids and Surfaces A: Physicochemical and Engineering Aspects 698 (2024) 134527

Contents lists available at ScienceDirect

Colloids and Surfaces A: Physicochemical and Engineering Aspects

journal homepage: www.elsevier.com/locate/colsurfa

# Influence of structural organization on mucoadhesive properties of poloxamer-hyaluronic acid-based micelles and hydrogels: From molecular modelling to biointerfaces interactions

Anderson Ferreira Sepulveda [a], Jéssica Bassi da Silva [b], Marcos Luciano Bruschi [b], Margareth KKD Franco [c], Fabiano Yokaichiya [d], Giovana Radomille Tófoli [e], Cíntia Maria Saia Cereda [e], Anabella Patricia Rosso [a], Fernando Carlos Giacomelli [a], Ana Ligia Scott [f], Daniele Ribeiro de Araujo [a,g,*]

[a] Centro de Ciências Naturais e Humanas, Universidade Federal do ABC, Santo André, São Paulo, Brazil
[b] Laboratory of Research and Development of Drug Delivery Systems, Department of Pharmacy, State University of Maringa, Maringa, Parana, Brazil
[c] Instituto de Pesquisas Energéticas e Nucleares—IPEN, São Paulo, Brazil
[d] Department of Physics, Federal University of Parana, Curitiba, Parana, Brazil
[e] São Leopoldo Mandic Faculty, São Leopoldo Mandic Research Institute, Campinas, São Paulo, Brazil
[f] Centro de Matemática, Computação e Cognição, Universidade Federal do ABC, Santo André, São Paulo, Brazil
[g] Department of Biophysics, Paulista Medical School, Federal University of Sao Paulo (UNIFESP), Sao Paulo 04023-062, Brazil

## GRAPHICAL ABSTRACT

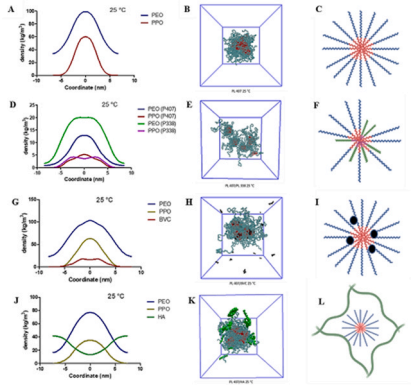

## ARTICLE INFO

*Keywords:*
Poloxamers
Hyaluronic acid
Micelles
Hydrogels

## ABSTRACT

New pharmaceutical formulations have been proposed as strategies to improve transport and provide best conditions to control the drug release rate in specific biological environments, such as mucosa surfaces. Herein, formulations containing binary systems Poloxamer (PL) 407 15 % and PL 338 15 %, combined with hyaluronic acid, carrying the local anesthetic bupivacaine (BVC), were studied by molecular dynamics, while other structural parameters were determined by Dynamic Light Scattering for stablishing relationships with mucoadhesive

* Corresponding author at: Department of Biophysics, Paulista Medical School, Federal University of Sao Paulo (UNIFESP), Sao Paulo 04023-062, Brazil.
*E-mail address:* draraujo2012@gmail.com (D.R. de Araujo).

https://doi.org/10.1016/j.colsurfa.2024.134527
Received 20 February 2024; Received in revised form 26 May 2024; Accepted 11 June 2024
Available online 12 June 2024

Structural organization
Mucoadhesion

properties and cytotoxicity evaluation. The binary system PL 407 15 %/PL 338 15 % exhibited a well-organized structural morphology, with more hydrated corona, and increased mucoadhesive properties over mucin layers. After hyaluronic acid (HA) incorporation, it was observed an increase on the force of detachment, possibly due to HA role as a linker among mucin layers independently of PL supramolecular structures. On the other hand, the addition of BVC or HA/BVC into the binary system decreased the force of detachment, as a response of augmented of compactness of these hydrogels caused by desolvation of PO core, showing the influence of all components and their chemical interactions into the structural organization and their biopharmaceutical performance relationships.

## 1. Introduction

Hydrogels based on synthetic and natural polymers have been extensively studied as materials of innovative pharmacological, cosmetical, agricultural and industrial importance, due to their structural and mechanical features [1–3]. It is well demonstrated that those hydrogels systems can perform additional biological functions, attributed to their components, as well as to control drug or bioactive molecules release, incorporated into their network architecture [3,4]. In addition, some of them are responsive to temperature, pH, light, for example, whose structure can be organized or disorganized according to environmental stimuli or even after incorporation of some additives such as drugs, salts, other polymers or nanocarriers. In this sense, herein we investigated relationships among poloxamer-based (PL) hydrogels composition, their structural aspects and how those features can impact on their biological properties after incorporation of other bioactive molecules.

PLs are thermosensitive polymers, composed of polypropylene oxide (PPO) and polyethylene oxide (PEO) chains arranged as PEO-PPO-PEO scheme, widely used as drug-delivery matrices due to their ability for self-assembly in micelles and then in hydrogels according to certain conditions, such as increased concentration and temperature. In special, the PL self-aggregation process is driven by inherent structural and physico-chemical properties since when PL chains are dispersed in water, they start to aggregate in micellar structures, as function of polymer concentration – higher than critical micellar concentration (CMC) and environmental temperature – higher than critical micellar temperature (CMT) [2,5,6].

In fact, CMC and CMT are intricated properties that involves thermodynamics and structural aspects. For example, first reports in the literature [7,8] studied the PL self-assembly mechanisms highlighting the dependence on temperature and PL concentration in solution, by comparing CMT and CMC values among PL and other nonionic surfactants. The micelles formation is resulted from polarity changes into the medium (caused by a temperature increase), evoking the aggregation of PEO and PPO blocks. This effect can be observed by calorimetric analysis being an endothermic phenomenon, with enthalpy values determined by PL type, molecular weight and PEO:PPO relationships, in response to PPO units dehydration and possible water molecules movement towards the PEO corona. Simultaneously to thermodynamics parameters, micelles solutions can be investigated by several techniques, such as DLS, SLS, scattering techniques (SANS and SAXS), rheology, providing essential structural information (micellar dimensions, interplanar distances and phase organizations).

The micellar core is highly dehydrated compared to corona and increments on temperature favor non-covalent interactions among PPO chains. Consequently, a physical process, involving the movement of more water molecules in direction the micellar corona, lead to the hydrogels formation. In this case, a combination of high PL concentration and temperature evokes the micelles aggregation as lyotropic liquid crystalline phases, assuming new reversible phase organizations, such as lamellar, cubic and hexagonal structures. The relationships among these supramolecular structures end up promoting different mechanical behaviors in the hydrogel, influencing on material rheological features, as viscosity, elasticity, rigidity, and specially on adhesion to biological surfaces, such as mucosa for example [3].

It is observed that hydrogels with high viscosity and strong polymeric interactions tend to have cubic and hexagonal supramolecular structures, depending on physico-chemical properties and polymer concentration. Additionally, these features also affect the drug release mechanisms and biopharmaceutics properties, influenced by the entanglements among polymeric chains, incorporation of salts, drugs and other additives. Indeed, high structured hydrogels based have presented high elasticity and consistency, structural stability, and adequate drug release performance, due to presence of cubic and hexagonal supramolecular structures in these hydrogels [9].

Hydrogels have been investigated due to their useful mucosal formulations, low-toxicity, and efficiency in controlling drug release for a prolonged time, and reducing side effects [10,11]. Polymeric chains can create entanglements with mucus, promoting enhanced interaction between the components of formulations and biological tissues, allowing prolonged residence time over application site [12]. This interaction between a hydrogel and a biological substrate defines the bioadhesion phenomenon [12]. In this sense, some mechanisms can explain it: (i) in contact to the mucus, the adhesive materials are hydrated and swelled, so non-covalent bonds with mucus molecular components take place; (ii) these materials diffuse towards the mucus, closely interacting with the mucosal components and consolidating the adhesive interactions [12–15].

Human mucus is formed by components that promote high viscosity, containing approximately 98 % water, 0.9 % salts, 0.8 % globular proteins, and 0.3 % high-molecular weight protein mucin polymers. Mucin forms a polymeric network with large number of physical entanglements, due to its covalent and non-covalent bonds. Glycosylation on mucin features a bottlebrush-like structure, so promoting stiffness and radius of gyration of mucin chains alterations [16,17]. Mucin gel presents a strongly negative charge at neutral pH, because of terminal sulfation and the presence of sialic acid, conferring stability via repulsive forces [16,17]. Mucin gels are viscoelastic materials with high elastic behavior ($G' > G''$), whose mucin concentration and cross-linking are highly regulated by $Na^+$ and $Cl^-$ balance in extracellular matrix. It can be altered when occurs some ionic imbalance in a mucus gel with lower elastic and viscous modulus, increasing molecular diffusion efficiency [17]. For human airway mucus, there are two principals synthetized and secreted mucins, MUC5B and MUC5AC, which are very large polymers (ranging from 0.2 and 10 μm) interweaving to show mesh-like gels [18]. In healthy persons, the balance between $Na^+$ absorption and $Cl^-$ secretion by epithelium hydrates adequately airway surfaces and promotes efficient mucociliary clearance. However, the imbalance of ion transport and the hypersecretion of mucin increase the mucin concentration in the mucus layer, decreasing mucociliary clearance. The transport and biophysical properties of mucus, such as osmotic pressure, adhesion, cohesion, and friction, are relatively affected by small variations in mucin concentration. It is clearly observed that higher concentration of mucin greatly diminishes transportability [18].

In this study, we assessed the influence of micelles and hydrogels structural aspects on their biopharmaceutics properties considering the formation of a PL-based binary system, composed of PL 407 and PL 338. Both Poloxamers have presented as excellent hydrogel drug-carriers for

treatment of articular issues, since their low toxicity and well-organized hydrogel in physiological temperature, allows to incorporate hydrophobic drugs which good structural stability [4,9,19]. PL 407 is formed by $EO_{98}$-$PO_{67}$-$EO_{98}$, while PL 338 by $EO_{46}$-$PO_{16}$-$EO_{46}$ structure, which causes difference on hydrophobic/lipophilic balance (HLB) between both polymers. This is reflected by EO:PO ratios of PL 407 and PL 338: while PL 407 has ratio of 3:1, PL 338 has 5:1. So, PL 338 is more hydrophilic than PL 407 with HLB = 27, against 22 for PL 407 [9].

Formulations incorporating polymers like PL 407 or PL 338 have demonstrated the ability to regulate drug release rates, especially for medications such as levofloxacin to combat multi-resistant bacteria [20] or lidocaine, ropivacaine, and bupivacaine for postoperative pain management in arthroplasties [4,9,19]. As shown in previous work [9], formulations of PL 407 15 %/PL 338 15 % (w/v) demonstrated high structural organization with high viscosity, high resistance, and elastic modulus comparable to PL 407 30 % (m/v). Indeed, it is demonstrated that this binary formulation also present coexistence of cubic and hexagonal supramolecular structures as well in PL 407 30 % (m/v) (as observed by Small-Angle Neutron Scattering), however the presence of PL 338 diminishes material stability under frequency or shear variation. As pointed by SANS results, binary systems present higher anisotropy than PL 407 30 % formulations, indicating that the presence of a more hydrophilic component diminishes the interactions among supramolecular structures [9].

The addition of more hydrophilic polymers can alter viscosity and increase adhesion on biological surfaces. For example, hyaluronic acid (HA) has been used to develop high viscosity materials [21–23] and promote the reinforcement of gel structure although it was not significantly altered thermosensitive self-assembling process [9,22]. Mayol and coworkers (2008) showed that presence of HA in PL 407 hydrogel enhanced interaction between gel and mucin, with a controlled and prolonged release of acyclovir [22]. Those properties can be attributed to the presence of (1→4)-β linked D-glucoronic and (1→3)-β linked N-acetyl-D-glucosamine residues as well as the OH groups deprotonate in physiological pH, conferring to HA a negative-charge and a strong polar characteristic.

Despite some systems containing both PL have been studied before, there is still a lack of molecular and mechanical characterization of PL 407/PL 338/HA hydrogels and their relationship with biological properties. The types of molecular interactions (hydrophobicity, hydrogen bonds, presence of charges) involved in micelles and hydrogels structural organization are responsible for modifications in mechanical properties and how those material can interact with biological surfaces. Sepulveda and coworkers (2023) demonstrated that the presence of hydrophilic polymers PL 338 and HA promoted better control on the release of bupivacaine hydrochloride (BVC) [9], since BVC diffusion is significantly affected by polymeric entanglement. Furthermore, adding PL 338 or HA can hinder BVC release, perhaps due to a second polymeric matrix, composed by HA chains, around supramolecular structures. The presence of HA seems not alter the type of supramolecular structure nor the lattice parameters, indicating that HA is a structuring agent among supramolecular structures.

BVC is local anesthetic widely used intraoperative and postoperative pain relief. BVC is hydrophobic drug that acts by blocking sodium channels, but the application of free BVC is related to diminished duration of anesthetic effects and to cardiac toxicity in high concentration [1,9]. To avoid these side effects, hydrogels have been proposed to develop the best materials for drug release control and decrease overexpose to anesthetic.

In this sense, this work aims to characterize the structural organization structure of micelles formed by PL 407, PL 338, and HA in the light of coarse-grained (CG) simulations for evaluating the microstructural organization of binary systems and their relationship with experimental approaches, as like hydrodynamic diameter, polydispersity, hydrogels mucoadhesive properties, and their cytotoxicity in the presence of additives such as HA and bupivacaine hydrochloride (BVC), used as drug model in this study.

## 2. Materials and methods

### 2.1. Materials

Poloxamers 407, 338 and mucin type II from porcine stomach (Sigma-Aldrich, Chem. Corp. Saint Luis, MO, USA) and HA (98.5 % purity, 150 kDa; Viafarma Ind. Farmc., São Paulo, Brazil) were used as formulations components. BVC hydrochloride (Pharmaceutical grade), used as drug model, was kindly received from Cristália Produtos Químicos Farmacêuticos LTDA (Itapira, São Paulo, Brazil). All salts and solvents were analytical grade.

### 2.2. Micelles and hydrogels preparation

Poloxamer 407 (PL407) as unique or binary systems with poloxamer 338 (PL338) at 5 % (w/v) PL final concentration were prepared in ultrapure water in the presence or absence of bupivacaine hydrochloride (BVC, 0.5 % w/v) and/or hyaluronic acid (HA, 0.5 % w/v). Similarly, PL-based hydrogels were prepared by drug dispersion (0.5 w/v %) in solutions of PL 407 (15–30 % w/v P15 and P30, respectively), or in association with 0.5 % w/v HA, and/or PL 338 (15 % w/v). All samples were maintained in cold bath under magnetic stirring until polymer solubilization and transparency. Samples were stored at 8 °C until use.

### 2.3. Molecular Dynamics studies by Coarse-Graining method (CG)

The micelle structural organization was studied through molecular dynamics by using the Coarse-Graining (CG) method. Parameters and mappings for PL 407, PL 338, HA, and BVC were established based on prior research (Fig. 1 A) [24–26], detailed in Tables S1, S2, S3 within the Supplementary Material.

Configurations were determined using Packmol software [27] within a 30 ×30×30 nm cubic box, randomly placing all molecules. Herein, it was performed five simulations for each system, varying the number of molecules (n): (1) PL 407 (n = 20 molecules), (2) PL 407 (n = 10 molecules) + PL 338 (n = 25 molecules), (3) PL 407 (n = 20 molecules) + HA (n = 100 molecules), and (4) PL 407 (n = 20 molecules) + BVC (n = 100 molecules). Each system was set up to 5 % concentration of PL, and simulations were carried out at both 25 °C (298 K) and 37 °C (310 K) temperatures, over 1.0 μs durations.

The CG models were developed by using the MARTINI 2 Force Field [24], and simulations by Gromacs 4.5.4 software package [28]. Anti-freezing water was employed as solvent, considering a time step of 20 fs, and every 200 fs, for non-bonded interactions [29]. Additionally, dispersion interactions and a shift function (starting point from 0.9 nm and a cutoff at 1.4 nm) were utilized.

In attempt to equilibrate all chains, an isothermal-isobaric (NPT) ensemble was employed at 25 ºC (298.15 K) and 37 °C (310.15 K), utilizing a Berendsen thermostat (coupling time of 0.5 ps). Other parameters such as Berendsen barostat (reference pressure of 1 bar, a coupling time of 4.0 ps, and compressibility of $3 \bullet 10^{-6}$ $bar^{-1}$) were used throughout the simulations [29].

Gmx polystat and gmx programs were employed to analyze the micellar structures [24,30,31], specially to compute metrics such as the radius of gyration (Rg, parameter referred to the molecules conformational fluctuation over time) and the end-to-end diameter (Ree, the longest distance covered by a molecule within a given segment) [32].

Rg was calculated by Eq. 1:

$$R_g = \sqrt{\frac{1}{N}\sum_{i=1}^{N}(\boldsymbol{r}_i - \quad \boldsymbol{r}_{cm})^2} \tag{1}$$

where $N$ represents the number of pseudoatoms, $\boldsymbol{r}_i$ denotes center of

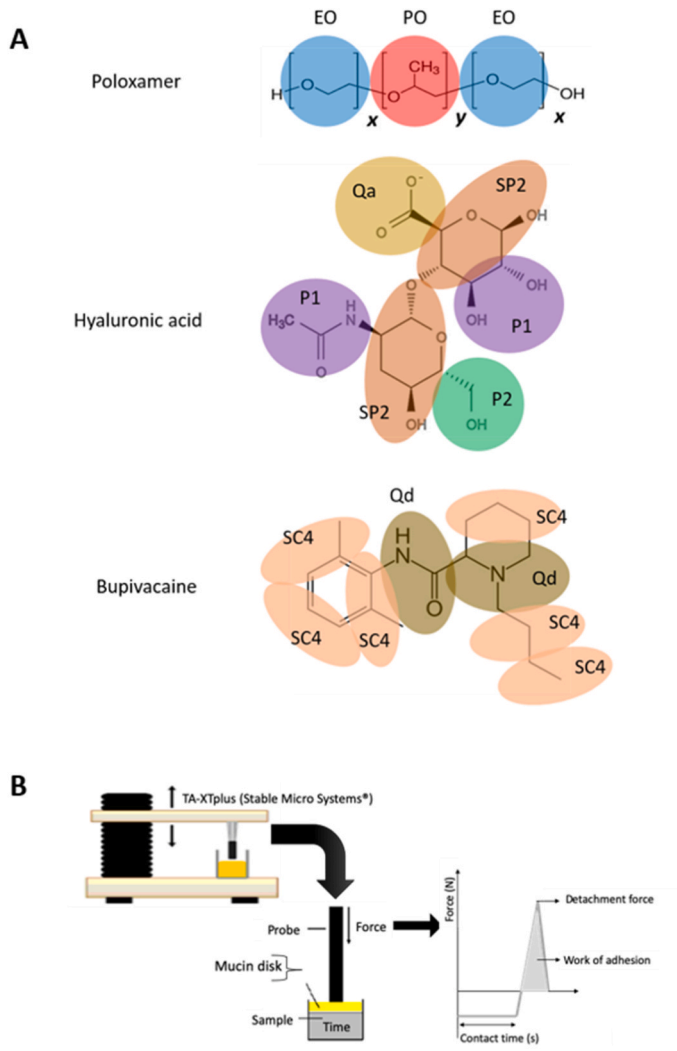


**Fig. 1.** (A) Coarse-grained molecules of Poloxamer, composed by *y* blocks of poly(ethylene oxide) – EO - and flanked by *x* blocks of poly(propylene oxide) – PO -, hyaluronic acid, and bupivacaine. (B) TA-XTplus texture analyzer and typical force vs. curve. time of the in vitro mucoadhesive profile.

mass position, and $\boldsymbol{r}_{cm}$ signifies the micellar center of mass. Low $R_g$ values indicate folded conformation, while high values show unfolded micelle [33].

The impacts of HA and BVC into the systems structure were analyzed considering temperature changes and the micelles solvent-accessible surface areas (SASA). All analyzes were performed by using the gmx sasa program [34,35] (Eq. 2).

$$\mathscr{A} = 4\pi\sum_i r_i^2 \frac{m_{acc}(i)}{m} \tag{2}$$

where $m_{acc}$ is the number of dots on pseudoatom *i* that is not hidden by neighboring elements.

### 2.4. Dynamic and Static Light Scattering (DLS and SLS) assays

The micellar hydrodynamic diameter and size distribution were determined by using the Dynamic Light Scattering (DLS) technique [36,37]. Samples were assessed by using a NanoSeries ZS90 particle analyzer from Malvern® Instruments. Measurements were conducted at an angle of 173º (at 25 and 37 ºC) [4,19], and samples were prepared at 5 % PL, in the presence and absence of additives like HA and BVC (at least 24 h prior to the analysis). Furthermore, simultaneous dynamic (DLS) and static (SLS) light scattering measurements as a function of concentration were conducted using an ALV/CGS-3 compact goniometer system. In such a case, light scattering data were acquired at scattering angle from 40° to 150°. The DLS data were analyzed using the Cumulant method to obtain values of relaxation frequency ($\Gamma = 1 / \tau$) related to the diffusion of the scattering particles, whereas the Debye plot was used to analyze the SLS data.

### 2.5. Mucoadhesive force analysis

The mucoadhesive properties of the hydrogels were assessed using the TA-XTplus texture analyzer (Stable Micro Systems, Surrey, England), in tension mode. The detachment force and the work of adhesion were evaluated, throughout the force and work required to remove the formulation from a mucin disc (Fig. 1B).

Firstly, the mucin disk was prepared by compressing powdered mucin (250 mg), using a compression ring with a diameter of 14 mm and a compression force of 10 tons, applied for 30 s [38–40]. The substrate (mucin disc) was horizontally fixed to the lower end of the texture profile analysis probe. Prior to testing, the mucin disk was hydrated in 5 % (w/w) aqueous mucin solution (using ultrapure water) over a period of 30 s. The excess liquid on the disk surface was removed by using a soft absorbent paper. At 37 °C, the formulation, previously packed in a cylindrical and shallow glass vial, was placed over the analytical probe, which was lowered until the mucin disk reached the surface of the sample. A contact force of 0.03 N was applied for 30 s, which kept the substrate just in contact with the hydrogel surface [40]. The probe was, then, raised with a constant rate of 10.0 mm/s, until complete detachment of the adhesive hydrogels from the mucin disks. The maximum force of detachment and the work of adhesion, which is the calculated area under the force/distance curve (Fig. 1B), obtained by the Texture Exponent 3.2 software (Stable Micro Systems). All the measurements were performed in at least three replicate samples of each formulation.

### 2.6. Cell viability assays

Balb/c fibroblasts (3T3 cells line) were used as models for evaluating the cytotoxicity evoked by all formulations and their components. Cells were seeded in 96 wells plates ($2.10^4$ cells/well) by using DMEM medium (Gibco Laboratories, Grand Island, NY, USA), supplemented with 10 % (v/v) fetal bovine serum (pH 7.2–7.4) and 100 µg/mL of penicillin/streptomycin and maintained in 95 % $O_2$ and 5 % CO atmosphere, at 37 °C, until reaching 80 % of confluence. Culture medium was changed every 48–72 h. For cell viability assays, formulations were evaluated by using indirect test according to ISO 10993–5 (2009) and cells treated during 24 h with different drug (0.625–18.75 µg/mL) and polymers (0.2–6 mg/mL) concentrations. Cell viability percentage was determined by MTT reduction test.

## 3. Results and discussion

### 3.1. Coarse-grained simulations

Systems simulations were conducted by Coarse-Grained (CG) representing groups of atoms as single interaction sites, reducing the computational complexity while preserving essential features of the system [29,30,41,42]. Notably, CG simulations applied to PL have exhibited results closely aligned with both all-atom simulations and experimental data [24,29,43], validating the use of CG simulations as reliable tools for exploring molecular and structural characteristics of PL-based systems. Moreover, CG simulations can be useful to reveal the capacity of PL to form micelles and to incorporate drug into their structures [43].

The calculated densities and enthalpy parameters, as shown in Tables S4 and S5 respectively, indicated the successful design of the

simulated systems, closely aligning with experimental values [9]. PL respond to temperature fluctuations due to the equilibrium between the enthalpy contribution (energetic stabilization via hydrogen bonds) and the system's entropy as temperature rises [44]. Each formulation exhibited an endothermic behavior, with enthalpy increasing with both complexity and temperature (Table S5). This increase suggests the promotion of micellar organization in response to the incorporation of additives, as observed in the PL 407/PL 338 and PL 407/BVC systems.

However, in the case of PL 407/HA, low enthalpy values were observed, indicating interactions between water molecules and the hydroxyl groups from PL 407 chemical structure. Similar interactions were expected to occur with HA's hydroxyl groups, conferring a highly hydrophilic nature to the system. These interactions play a pivotal role determining the system's behavior considering distinct influence of additives on the micellar organization.

The high enthalpy values observed in the PL 407/PL 338 system can be attributed to intricate interactions between the PL 407 and PL 338 chains, like the dynamics observed in the PL 407/BVC systems. In the case of PL 407/PL 338 binary system, the system's complexity tends to increase due to the micellar corona solvation, driven by the incorporation of PL 338, which is more hydrophilic than PL 407. This increased hydrophilicity can enhance the interactions and complexity within the system, leading to higher enthalpy values.

Despite BVC is a hydrophobic molecule, its addition as hydrochloride salt form, evokes changes on micelles arrangement. For example, while the drug can be interacting with the micellar core, the salt interacts with the hydrated corona, evoking a salting-out effect, as also previously described [3,19,32,45].

The Rg values for EO and PO segments (PL 407, PL 338) are displayed in Fig. 2A and detailed in Table S6. Despite the linkage between EO and PO segments within PL 407 and PL 338 (Fig. 1 A), their Rg values agree with that reported in the literature [29]. Interestingly, at 25°C, the EO segments of PL 407 chains exhibit greater compactness (Rg = 3.67 nm) when compared to those from PL 338 (Rg = 2.6 nm), reflecting higher dynamic stability of PL 338 EO segments than PL 407 EO segments [43]. However, the Rg of EO segments within PL 407 becomes less stable in the presence of BVC or HA at the same temperature (Rg = 4.5 nm and 3.8 nm, respectively). Furthermore, the EO segments of PL 407 become more compact in the presence of PL 338, BVC, or HA.

These variations in the Rg values of PO segments can be explained by the hydrophilic nature of PL 338 and HA. Their hydrophilicity likely facilitates increased interactions with the PO segments of PL 407, limiting the expansion of these EO chains. However, in the presence of BVC, interactions with the PPO core can be favored by the hydrophobic character of the BVC molecule, leading to the observed differences in the Rg values of PEO segments.

Results from our study showed insignificant change in PL 338 Rg values at 37 °C. However, for PL 407 chains, a slight decrease in Rg values occurs as temperature rises, consistent with previous findings [31]. At 37°C, the Rg values for both EO and PO segments of PL 407 decreased (from 3.67 nm to 3.62 nm for PEO and from 1.6 nm to 1.2 nm for PPO). In contrast, PL 407/PL 338 and PL 407/BVC systems at 37°C revealed Rg increasing, likely due to stronger molecular interactions, particularly within the PPO core.

While PL 407 chains tend to exhibit decreased Rg values with temperature raised, other systems showed a slight decrease in Rg at 37 °C. PL 407/PL 338 maintained a low variation in Rg throughout the simulation, indicating minimal conformational changes in both PL 407 and PL 338 chains at 25°C. In comparison, PL 407/BVC and PL 407/HA systems displayed higher Rg variation (for both EO and PO segments) compared to PL 407/PL 338. This effect suggests possible impacts of BVC and HA on PL chains conformations. Notably, the less variation in EO chains Rg in PL 407/HA may indicate some interaction between HA and EO segments, potentially influencing chain conformations.

The end-to-end distance (Ree) parameter (Fig. 2B and Table S7) showcased how the presence of PL 338, BVC, or HA influenced the conformation—compressed or extended—of PEO and PPO chains. The Ree values for the EO segments of PL 407 increased in the presence of BVC (Ree = 11 nm at 25°C) or HA (Ree = 9.0 nm at 25°C), while the PO core exhibited lower Ree values in the presence of PL 338, BVC, or HA. These observations suggest a potential promotion of increased hydrophobic interactions among PO blocks, due to the incorporation of salts and other additives [46]. Conversely, the presence of PL 338 decreased the Ree value (5.92 nm at 25°C) of PEO blocks within PL 407. This decreased Ree value indicated a structural change in the micellar corona, forming U-shaped PEO chains due to the influence of PL 338 [46].

In the PL 407/PL 338 system, there's a coexistence of micelles comprising separate PL 407 and PL 338, as well as associations between both PL types. Molecular simulations experiments revealed that the PL 407 and PL 338 chains tend to aggregate (Fig. 3D-F) while the binary system exhibited a more complex configuration compared to micelles composed of a single PL type (Fig. 3A-C). At 25°C, both EO and PO segments of PL 338 were oriented toward the corona and core surfaces, respectively. At 37 °C, to reduce entropy (Table S5), the EO segments of PL 338 still partially surface the corona, while the PO segments tend to

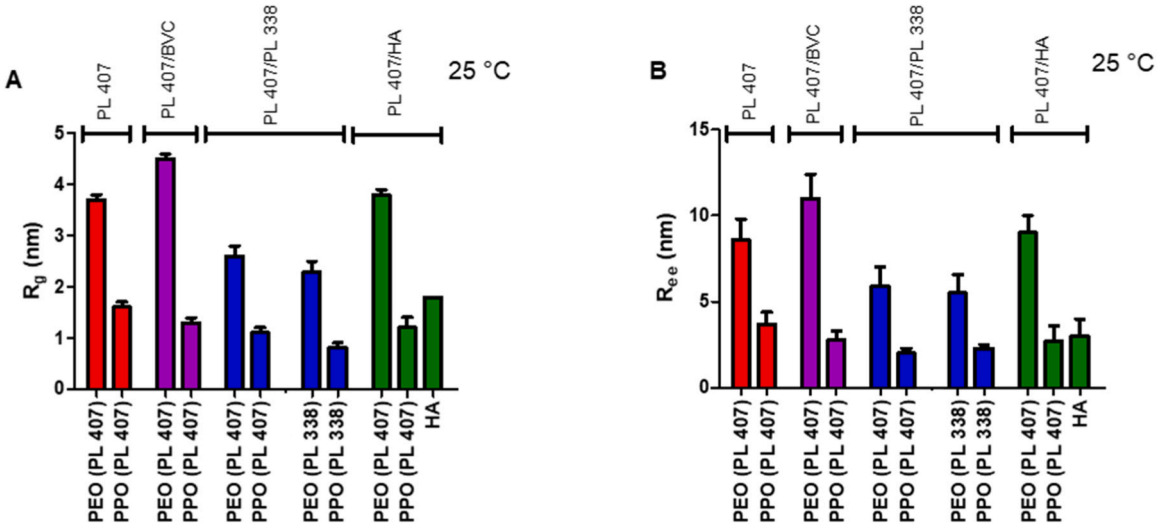


**Fig. 2.** Plots of radius of gyration (A) and end-to-end distance (B) of chains of poly(ethylene oxide) (PEO), poly(propylene oxide) (PEO), and hyaluronic acid (HA) obtained from molecular dynamics of micellar structures of PL 407, PL407/BVC, PL 407/PL 338, and PL 407/HA after 1 ms of simulations (n = 4). BVC: bupivacaine.

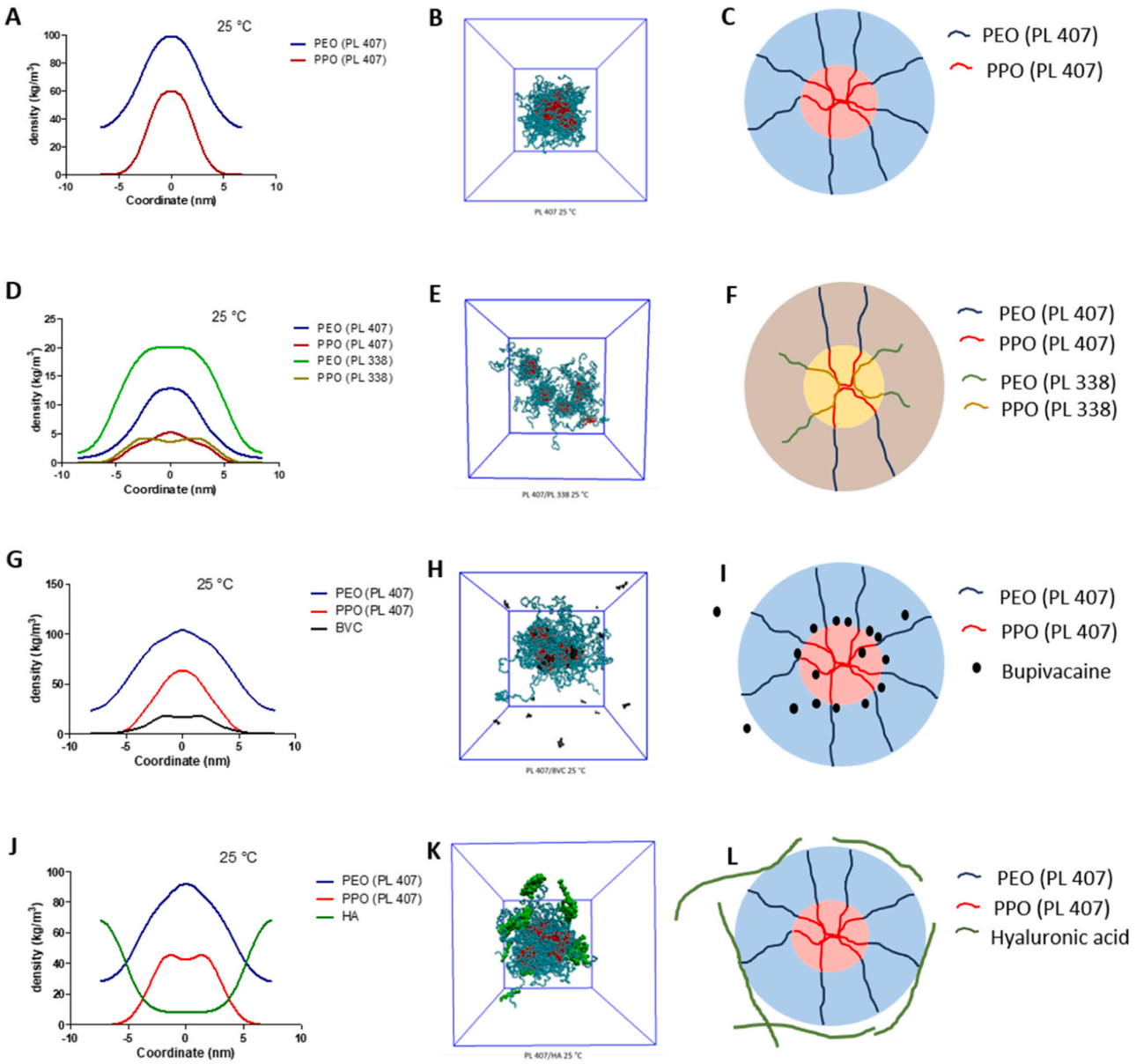


**Fig. 3.** Density distributions (kg/m$^3$) of PL 407 (A), binary system PL 407/PL 338 (D), PL 407/BVC [bupivacaine] (G), and PL 407/HA [hyaluronic acid] (J), after 1 microsecond of simulation at 25 °C (273 K). Snapshots (at moment 1 μs) are shown respectively for each system: PL 407 (B), binary system PL 407/PL 338 (E), PL 407/BVC (H), and PL 407/HA (K), where cyan beads are EO (ethylene oxide) blocks, red beads are PO (propylene oxide) blocks, black molecules are bupivacaine, and green beads are hyaluronic acid components. Micelles schemes, based on simulation results, are shown in: PL 407 (C), binary system PL 407/PL 338 (F), PL 407/BVC (I), and PL 407/HA (L), where blue lines are PEO chains of PL 407, red lines are PPO chains of PL 407, orange lines are PPO chains of PL 338, dark green lines are PEO chains of PL 338, black dots are bupivacaine molecules, and light green lines are hyaluronic acid chains.

blend into the core. Despite its complexity, the PL 407/PL 338 micelle demonstrates a lower partial density compared to the PL 407 micelle alone. This intricate relationship between the two PLs suggests interactions that might not be as rigid as those observed in the PL 407, PL 407/BVC, and PL 407/HA systems (Fig. 3).

The BVC incorporation into the PL 407 systems did not alter the micellar structure; rather, the overall structure remains comparable to the system without BVC. BVC molecules tend to incorporate into the core due to their hydrophobic nature, interacting predominantly with the PO blocks (Fig. 3G-I). The amine group within BVC molecule, being more hydrophilic, shows a tendency to interact with the EO block. Similarly, HA exhibits interactions with both water molecules and the EO blocks of PL.

In the simulated PL 407/HA system, the HA chains envelop the micelle entirely as a polymeric matrix (Fig. 3J-L), as our previous work theorized [9]. Unlike the other systems, this configuration maintains the micelle's organization, yet the PO core appears more expanded compared to the other systems depicted in Fig. 3. Interestingly, despite this expansion, the end-to-end distance values of the PO blocks in this system are not substantially greater than those observed in other configurations (Table S7).

The PL micelles behavior, in response to temperature changes, involves a self-assembly process driven by micellar core dehydration, leading to enhanced interactions among the EO blocks. Upon increasing the temperature to 37 °C, there is a slight decrease in the accessible area from the EO blocks to water molecules, reducing from approximately 1140 nm$^2$ to 1020 nm$^2$. However, there is a minimal variation in the surface area of the core with temperature, indicating the stability of the corona itself.

In contrast, the PL 407/PL 338 system exhibits a more intricated

behavior compared to PL 407 alone. Within the conjugated micelle, the PL 338 portion behaves similarly to PL 407 micelles. The corona with the PL 338 EO blocks ranges from 450 $nm^2$ at 25°C to 400 $nm^2$ at 37°C, while the PO core remains unchanged. However, the PL 407 EO and PO blocks demonstrate higher responsiveness to temperature variation. At 25°C, the EO blocks of PL 407 have an accessible surface area of approximately 220 $nm^2$, which increases to just over 450 $nm^2$ at 37°C. Similarly, the PO core increased from 45 $nm^2$ to almost 75 $nm^2$. Given that PL 407 chains are longer than PL 338, despite PL 338 being more hydrophilic, since that the EO blocks of PL 407 are more exposed to water than those of PL 338, a scenario that might also hold true for the PO blocks. This exposure to water might contribute to the observed differences in the surface area changes with temperature between the two PL types within the PL 407/PL 338 system.

The addition of BVC to the PL 407 system notably impacts its micellar organization. In PL 407/BVC, the PEO blocks appear more exposed to solvent compared to PL 407, exhibiting an accessible area of approximately 2000 $nm^2$ (compared to just over 1000 $nm^2$ in PL 407). Interestingly, increasing the temperature does not significantly change this area value. Given that BVC molecules tend to bind to the core, it's expected that the surface area accessible to water would be smaller in micelles containing BVC. Indeed, the surface area of the PO core is approximately 250 $nm^2$ in the presence of BVC, while the core of PL 407 alone showed an area of 270 $nm^2$.

Meanwhile, the presence of HA increases the available area of the PEO corona compared to the PL 407 micelle without HA, reaching around 1400 $nm^2$ in PL 407/HA at 25 °C. However, with an increase in temperature to 37 °C, this area decreases to approximately 1200 $nm^2$ due to the interactions between HA chains and the EO blocks via hydrophilic interactions. Despite a slight distension observed in the core's partial density distribution in PL 407/HA, the accessible surface area to water remains relatively unchanged compared to the PL 407 system, maintaining a value of approximately 260 $nm^2$. These results indicate that adding HA can diminish micellar coalescence and then promote more polymeric interactions between HA and mucin chains, due to intercalation between polymer chains of HA and mucin [47–49].

Despite variations in micellar morphology, all systems exhibit stability at both 25°C and 37°C. The incorporation of PL 338, BVC, or HA chains alters the conformational model of micelles and interactions among molecules. Physico-chemical parameters like enthalpy values, radius of gyration, end-to-end distance, partial density distribution, and solvent accessible surface area provide a comprehensive description of structural changes influenced by different components and temperature variations within the micelles. The presence of hydrophilic components, such as PL 338 and HA, promotes higher hydration of the corona while restraining the extension of EO chains. On the other hand, BVC strongly interacts with the PO core, enhancing interactions among EO blocks and increasing the surface area accessible to water. Additionally, HA plays a role as a stabilizer of the micelle by interacting with EO block chains through hydrophilic bindings.

Overall, the incorporation of PL 338, BVC, or HA chains into the PL 407 system significantly alters the conformational model of micelles and their molecular interactions, as elucidated by various physico-chemical parameters characterizing the structural changes induced by different components and temperature variations. The different findings on simulated micelles are related to the molecular weights and sizes of the chains and the HLB of both Poloxamers: PL 338 is a heavier polymer (MW = 14600) and higher hydrophilicity with HLB = 27 than PL 407 (MW = 12600, HLB = 22), besides the critical micellar concentration (CMC) of PL 338 (CMC = 2.8 μM) is lower than that of PL 407 (CMC = 22) [9]. Thus, the presence of PL 407 micelles and PL 338 micelles separately can be explained by the possibility the PL 338 chains agglutinate in micelles in much lower concentration than PL 407, favoring the formation of PL 338 [50,51]. However, as pointed by our results, both PL 407 and PL 338 agglutinate into single micelles as time and/or temperature increases. Wu and collaborators (2020) simulated binary systems composed by different proportions of PL 407 and non-ionic surfactant HS15, where they propose that hydrophobic force leads the incorporation of HS15 molecules into PL 407 micelles, forming HS15 clusters inside the structure at least after 100 ns of simulation, although the aggregation process seems not get an equilibrated state within 1 μs [43], as did our mixed micelles. The authors argue that low PL 407 concentration could cause this low dynamic stability.

### 3.2. Hydrodynamic diameter and polydispersity: components influence on micellar dimensions

In general, micellar dimensions are influenced by formulations composition, predominantly driven by intermolecular interactions among their components. All samples displayed reduced hydrodynamic diameter when the experimental temperature was raised from 25 °C to 37 °C (Tables S8 and S9), influenced by micellar core dehydration. After the CMT, EO monomers become less hydrophilic, indicating an increasingly organized and complex polymeric network, indicated by unimodal curves in Fig. 4B and Table S8.

At 25°C, all PL samples exhibited bimodal distributions, due to the coexistence of fully formed micelles and 7 nm polymer unimers. The addition of HA seems not to modify greatly micelle diameter (with approximately 30 nm), which is similar to DLS results in [4], although other works points out bigger micelles or large aggregations due to presence of high molecular weight HA [4,10]. This discrepancy could be related to the incomplete micellization process.

Following BVC salt form incorporation, the micellar hydrodynamic diameter tended to decrease from 30 nm to 25 nm, induced by micellar core dehydration via salting out effect in both temperatures. Additionally, BVC hydrophobic molecule augmented the micelle hydrophobic character, resulting in increased water molecule release at physiological temperature. However, following HA incorporation, samples containing BVC slightly increased their micellar size compared to HA-free samples (~16 %) (Table S8), due to micellar aggregation caused by HA chains [10]. Indeed, for these particular systems, we have also performed DLS measurements as a function of concentration at 37 °C. In such case, the apparent diffusion coefficient ($D_{app}$) was calculated as:

$$D_{app} = \frac{\Gamma}{q^2} \tag{3}$$

where $q$ is the wavevector defined as:

$$q = \frac{4\pi n}{\lambda}\sin\left(\frac{\theta}{2}\right) \tag{4}$$

being $\lambda$ the wavelength of the incident light source (632.8 nm), $n$ the solvent refractive index and $\theta$ the scattering angle at which the light scattering detector was placed. The clearly visible $q^2$ dependence of the relaxation frequency ($\Gamma$) reported in Figures S1 representatively for PL sample in the presence of BVC and HA (PL/HA/BVC) indeed implies diffusive scattering particles regardless of the polymer concentration. This feature has been observed for all other investigated systems (not shown for brevity). The apparent diffusion coefficient ($D_{app}$) which is given by the slope of the linear $\Gamma$ *vs.* $q^2$ profiles is evidenced to be concentration-dependent and it systematically increases as concentration increases. The translational diffusion coefficient at infinite dilution ($D_0$) was accordingly determined using the following relation:

$$D_{app} = D_0(1 + k_D c) \tag{5}$$

where $k_D$ is the diffusion interaction parameter and $c$ is the polymer concentration. These data are provided in Figure S2 and the values of $D^\circ_H$ (hydrodynamic diameter at infinite dilution) were calculated using the determined values of $D_o$ *via* the Stokes-Einstein relation:

$$D_H^o = \frac{k_B T}{3\pi\eta D_O} \tag{6}$$

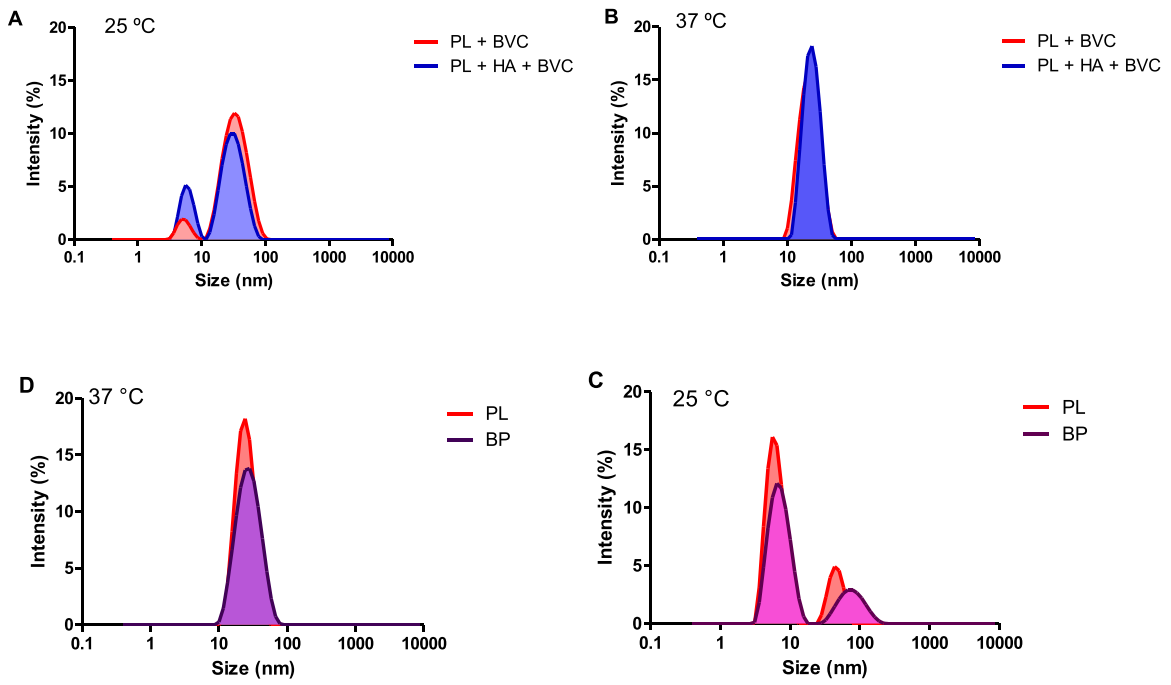


**Fig. 4.** Intensity profiles obtained from DLS experiments, as a function of size distribution (in nm) of PL 407 micelles with bupivacaine (BVC), with or without HA [hyaluronic acid] at 25 °C (A) and 37 °C (B), and PL 407 and binary system PL 407/PL 338 (BP) at 25 °C and 37 °C. All formulations for this measurement were prepared at 5 % (w/v) in water.

where $\eta$ is the viscosity of the solvent, $T$ is the absolute temperature and $k_B$ is the Boltzmann constant. These experimental data ($D_o$ and $D^\circ_H$) are reported in Table 1.

The values of $D^\circ_H$ (determined at infinite dilution) therefore confirms the increased size by HA incorporation in BVC-containing samples in the condition of non-interacting particles. Furthermore, by measuring the diffusion coefficient as a function of concentration, one notices qualitatively that $k_D > 0$ (the slopes are visually positive regardless of the sample as evidenced in Figure S2) suggesting accordingly repulsive polymer-polymer, therefore favourable polymer-solvent interactions. This feature indeed causes an apparent increase in $D_{app}$ and respective decrease in $D_{Happ}$ as the concentration increases.

Concerning the polydispersity indexes, the values for PL samples indicated moderate size dispersity (ranging from 0.25 to 0.36) at 25°C, commonly observed in some polymeric formulations. High PDI values, obtained from samples containing HA, suggest the formation of complex structures due to HA interacting with the hydrophilic micellar corona.

For binary PL-based systems (BP), physiological temperature also reduced micellar dimensions, with similar dimensions to those observed for unique systems before and after drug and/or HA incorporation, as shown in [10] (Table S9). BP systems showed less temperature-induced size variation compared to PL 407 systems, potentially due to the stabilizing role of PL 338, possessing a higher proportion of EO:PO and greater molecular mass. As temperature increased, PL 338 EO chains became more hydrophobic, while PL 407 EO chains retained water molecules. Neither drug nor HA significantly altered BP micellar dimensions, indicating relatively stable structures compared to one PL-type systems. This was also confirmed by the values of diffusion coefficient at infinite dilution ($D_0$) and the respective values of $D^\circ_H$ which are indeed very similar (Table 1).

Furthermore, we have probed the systems at physiological temperature by static light scattering. Since the particles are notably small (dimension smaller than $\lambda/20$ with $\lambda = 632.8$ nm), the angular dependent form factor can be neglected as representatively provided for the PL system at 5 % (w/v) in water in the presence of BVC with HA (Figure S3). Therefore, the molecular weight and the second virial coefficient ($A_2$) of the systems could be estimated by using the Debye equation:

$$\frac{Kc}{R_{\theta=90^\circ}} = \frac{1}{M_{w(mic)}} + 2A_2c \quad (7)$$

The Debye plots ($Kc/R_{\theta=90}$ as a function of the concentration) are given in Figure S4. The intercept of the profiles gives values of $M_{w(mic)}$ and the slope corresponds to the second virial coefficient ($A_2$) which describes purely thermodynamic the colloidal interactions. The profiles reported in Figure S4 also highlights repulsive polymer-polymer interaction and attractive polymer-solvent interactions as $A_2 > 0$ (positive slopes are clearly observed) thus causing an apparent decrease in molar mass (increase in $Kc/R_\theta$) as concentration increases. The values of $A_2$ reported in Table 1 are clearly higher for BP systems compared to the pure counterparts, thus confirming more favourable polymer-solvent interactions in the presence of the more hydrophilic PL 338 block copolymer in the formulation. Although the $k_D$ combines thermodynamic and hydrodynamic contributions, higher values of $k_D$ have been also determined for the binary systems as also reported in Table 1. Indeed, $k_D$ values measure by DLS typically correlates well with $A_2$ values measured by SLS.

The determined values of $M_{w(mic)}$ are equally provided in Table 1 and

**Table 1**
Structural features determined by simultaneous angular-dependent dynamic (DLS) and static (SLS) light scattering measurements at 37 °C for PL and binary system (BP) in the presence of bupivacaine (BVC) with or without hyaluronic acid (HA).

| Formulation | $D_o$ ($10^{-11}$ $m^2.s^{-1}$) | $D^o_H$ (nm) | $k_D$ ($cm^3.g^{-1}$) | $M_{w(mic)}$ ($g.mol^{-1}$) | $A_2$ ($mol.cm^3/g^2$) |
|---|---|---|---|---|---|
| PL/BVC | 3.05 | 21.5 | 6.30 | $1.51 \times 10^4$ | $3.33 \times 10^{-2}$ |
| PL/HA/BVC | 2.91 | 22.6 | 6.25 | $2.12 \times 10^4$ | $3.51 \times 10^{-2}$ |
| BP/BVC | 2.67 | 24.6 | 8.24 | $2.50 \times 10^4$ | $5.32 \times 10^{-2}$ |
| BP/HA/BVC | 2.64 | 24.8 | 7.58 | $5.19 \times 10^4$ | $4.74 \times 10^{-2}$ |

they in principle suggest higher molecular weight of the micelles produced using the binary systems. Nevertheless, we underline that the absolute values of $Kc/R_\theta$ depends on the refractive index increment of the scattering particle, which depends of the precise system composition (weight fraction of each component) and respective indexes of refraction. Accordingly, although determined values of $M_{w(mic)}$ agree with the DLS measurements to some extent (larger dimension are monitored for supramolecular aggregates with higher molecular weight) we underline that such absolute values may hold a fairy high degree of uncertainty due to the mentioned reasons.

Last but not least, distribution plots for PL and BP formulations, along with PDI numbers, displayed broader peaks for BP formulations than PL, suggesting the possibility of either combined polymer micelles or separate micelles composed of PL 407 and PL 338 within the binary systems, containing micelles with a broader size range, as well in [4] and in [54]. Although the tendency to form single micelles is visualized, the simulations carried out may have confirmed the presence and coexistence of PL 407 and PL 338 micelles and mixed micelles, at least during the simulation time (Fig. 3D-F). Both the addition of HA and PL 338 have a significant structuring role because of these differences in micellar microstructures, where both free HA and Poloxamer chains can serve as anchors on mucosal surfaces.

### 3.3. Mucoadhesive force analysis

In attempt to evaluate the influence of hydrogels compositions in mucoadhesive properties, in vitro adhesive force studies were performed for all formulations. All results are displayed in Fig. 5.

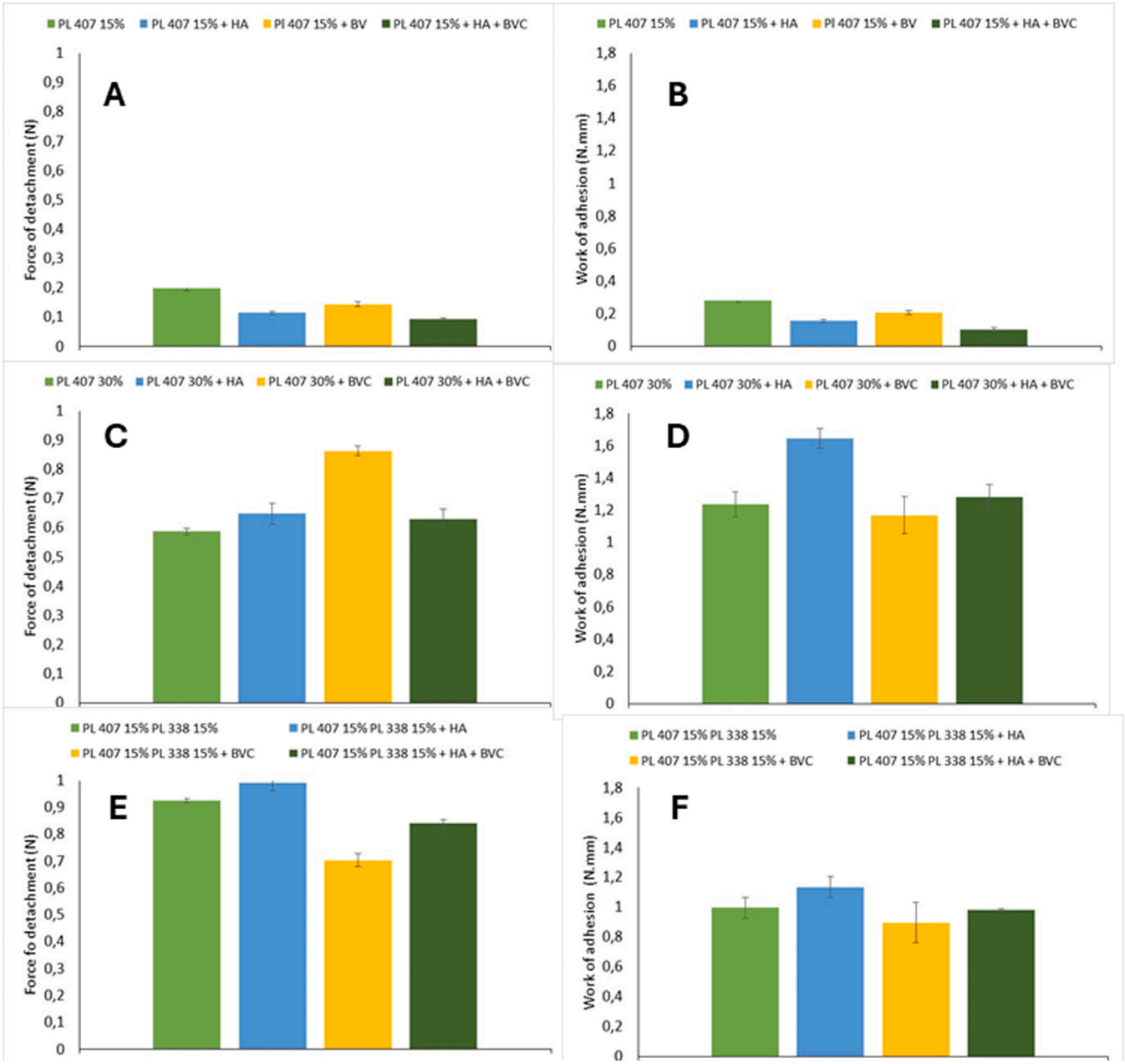


**Fig. 5.** Force of detachment (A, C, and E) and work of adhesion (B, D, and F) were performed to analyze mucoadhesive properties of PL 407 15 % (A and B), PL 407 30 % (C and D), and binary system PL 407/PL 338 systems (E and F), with hyaluronic acid (HA) and bupivacaine (BVC), in mucin. As Poloxamer concentration is increased, adhesive characters are also promoted due to enhanced interaction between PL and mucin chains. Additionally, the presence of HA also enhances this interaction because of non-covalent and hydrophilic bonds. PL 407 30 %.

As the total concentration of PL increased, it is observed a strong interaction among the polymer chains, reflecting a stiffer formulation, due to high number of non-covalent bonds or entanglements. It is proposed, by diffusion theory, that PL chains can diffuse into mucin layers [12,17,49,52], since these structures are smaller than 100 nm [17]. Fig. 5 shows that PL 407 30 % and PL 407 15 %/PL 338 15 % hydrogels demand higher force of detachment than PL 407 15 % (~ 3 or 4-times, respectively).

The presence of hydrophilic polymers, as PL 338 and HA, can affect the manner how the mucin-PL hydrogel systems interact. It is observed that HA chains exhibit the establishment of strong bonds with the mucin glycoproteins, since the detachment force of PL 407 30 %/HA hydrogel is approximately 10 % higher than that observed for the system without HA (Fig. 5C). A strong hydrogel-mucin interaction is observed for systems containing PL 338 chains, with a force of detachment 56 % higher than PL 407 30 % hydrogel (Fig. 5E). The addition of HA has slightly enhanced the interaction between binary systems and mucin, showing values from 0.92 N in PL 407 15 %/PL 338 15 % hydrogel to almost 1 N in PL 407 15 %/PL 338 15 %/HA.

In a previous study [9], it was shown that the addition of BVC can promote polymeric entanglements in both PL 407 30 % and PL 407 15 %/PL 338 15 %, leading the formation of a highly consistent hydrogel. As BVC is as salt form (BVC hydrochloride), its presence promotes the formation of non-covalent bonds among polymeric chains, by the dehydration process of PO cores (a phenomenon known as Hoffmeister effect). Therefore, an increased force of detachment is observed in PL 407 30 %/BVC system. In addition, in PL 407 30 %/HA/BVC is observed that the hydrogel has the same behavior of PL 407 30 %/HA; thus, hyaluronic acid chains act as anchor into mucin layers independently of supramolecular structures of poloxamer. However, the addition of BVC or HA/BVC into the binary system decreases the force of detachment, as a response of augmented of compactness of these hydrogels caused by desolvation of PO core.

As expected, increasing the total PL concentration from 15 % to 30 % conduced to a higher bioadhesive behavior (from approximately 0.2 N.mm to 1.4 N.mm – for PL 407 30 % systems – and to 1 N.mm – for PL 407 15 %/PL 338 15 % systems), because of high entanglement among poloxamer chains, high viscosity of the hydrogel and molecular interaction between poloxamer and mucin chains (Figs. 5B and 5D). Moreover, it was observed that the presence of HA promoted an enhanced work of adhesion (Figs. 5B, 5D, and 5E), as previously reported [16,18]. The low viscosity of the binary systems fosters low interaction among supramolecular structures [17], which can diminish the contact between mucin layers and hydrogel, demanding a low work to detach the formulation from the mucosa surface. As pointed by *in silico* results, 15/15 % PL 407/PL 338 systems contain, at the same time, hybrid PL 407 and PL 338 micelles, conferring a weaker material when compared to PL 407 30 % hydrogels. It is observed, by the high values of accessible surface to water in the binary micelles, that EO chains are more available to water interactions than the isolated systems.

When the HA is incorporated into the PL 407 30 % and PL 407 15 %/PL 338 15 % formulations, there was slight increasing in bioadhesive behavior, since its work of adhesion enhanced from 1.2 N.mm to 1.6 N.mm in PL 407 30 %. But PL 407 15 %/PL 338 15 %/HA showed similar result to binary system without HA, with approximately 1.0 N.mm. However, in systems containing BVC, the HA presence slightly increased the values from 1.2 N.mm (in PL 407 30 %/BVC) to 1.3 N.mm (in PL 407 30 %/BVC/HA), and from 0.9 N.mm (in PL 407 15 %/PL 338 15 %/BVC) to 1.0 N.mm (in PL 407 15 %/PL 338 15 %/BVC/HA) (Fig. 5). This significant change in work of adhesion ($p < 0.05$) in formulations containing bupivacaine can be related to a higher compactness of hydrophobic core, or more rigidity of polymer network because of augmented interactions between polymer-polymer and polymer-drug (as it is shown in Figure S5), that inhibits the interaction between mucin and formulation [19]. With our results, we demonstrate that binary system with HA present high adhesiveness onto mucin, being appropriate to reside over the mucosa by a prolongated period of time; however, PL 407 30 % hydrogels still presented improved mucoadhesive performance, but it is more consistent than binary hydrogels, have higher sol-gel transition temperature [9]. On the other hand, the addition of HA can promote increased bioadhesive behavior, but it diminishes consistency. In addition, binary formulations are significantly less consistent, decreased sol-gel transition temperature, and similar bioadhesion than PL 407 30 % systems. Systems with more viscous character, as PL 407 15 %/PL 338 15 % and PL 407 15 %/PL 338 15 %/HA, with sol-gel transition temperature close to ambient temperature, show higher diffusion rate in mucin gel and decreased contact to mucin network [17,52], being appropriate to pharmacological use.

### 3.4. Cytotoxicity studies

Results from Fig. 6 demonstrate the impact of various formulations, including polymers, HA, and BVC, on the viability of 3T3-fibroblast cell lines. Generally, treatments involving delivery systems with BVC did not significantly induce cytotoxic effects on cells, maintaining viability percentages above 60 %. However, reductions in cell viability percentage were observed only at high drug concentrations (12.5 and 18.75 μg/mL; $p < 0.001$).

Regarding the compositions, formulations containing HA exhibited higher cell viability percentages compared to those with PL407 and PL407/PL338, particularly within the 2–6 mg/mL polymer concentration range. This effect was similarly observed after BVC incorporation. Conversely, at the highest BVC concentration, PL407-PL338 demonstrated increased cell viability percentages compared to other formulations. This suggests a potential protective effect of PL407-PL338 formulation against BVC-induced cell damage.

These findings align with previous observations regarding PL407/PL338 formulations and their impacts on cell viability. Similar results

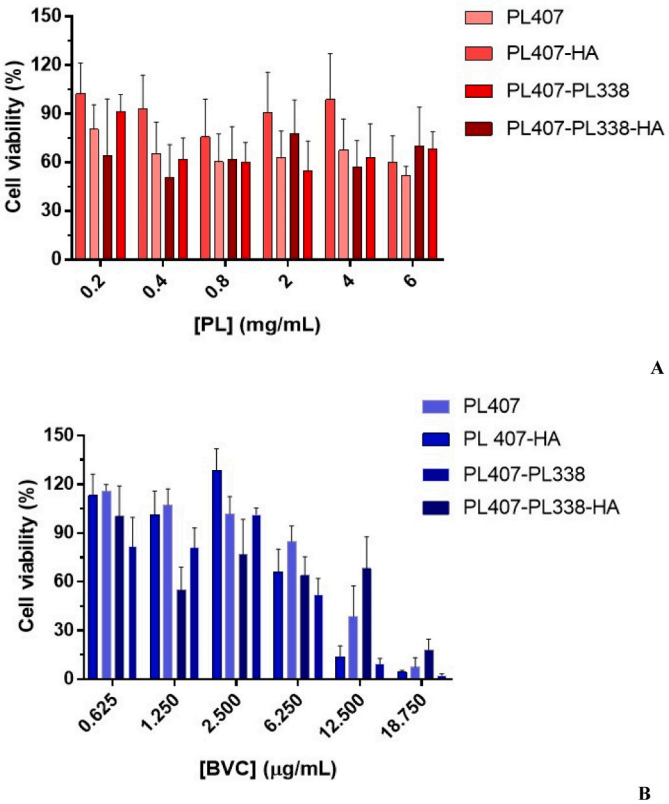


**Fig. 6.** Cell viability percentage evaluated by MTT reduction test in 3T3-fibroblasts. Poloxamer-hyaluronic acid systems cytotoxicity was assessed before (A) and after bupivacaine (BVC) (B) incorporation (n=3/concentration).

were reported for local anesthetic like lidocaine and ropivacaine in 3T3-fibroblast and Vero-kidney epithelial cell lines, respectively [4, 53–54]. Furthermore, the incorporation of anti-inflammatory agents, such as sulforaphane, in PL407-PL338 hydrogels has shown reduced cytotoxic effects in SW1353-chondrosarcoma and MC3T3-osteoblast cell lines [21].

Those findings highlight the versatility and potential applications of the PL407-PL338 hydrogel composition across different therapeutic purposes.

## 4. Conclusions

The development of pharmaceutical formulations combining different components has led to the creation of new delivery systems with unique structural architectures and significant impacts on their biopharmaceutical behavior. In this study, we focused on combining poloxamers, known for their thermosensitive properties, with hyaluronic acid, which offers bioadhesive characteristics. This combination resulted in systems capable of controlling both drug release rates and adhesion to mucosal surfaces.

We found that the structural organization within micelles are hydrogels are influenced by the type and concentration of each polymer used, as well as the incorporation of additives. When more hydrophilic polymers were added to the systems, their rheological properties were altered, such as viscosity, and enhanced their adhesion to biological surfaces, particularly noticeable in the presence of hyaluronic acid. Interestingly, hyaluronic acid seemed to strengthen the gel structure without significantly affecting the self-assembly process of poloxamers micelles. This fact indicated that while the components' self-assembly remained intact, their interactions with biological surfaces, especially mucin, were enhanced.

The addition of hydrophilic polymers like PL 338 and hyaluronic acid led to the formation of more complex systems compared to those based only on PL. Specifically, our study highlighted that a formulation of PL 407 15 %/PL 338 15 % exhibited a well-organized structural morphology, featuring a more hydrated corona in the binary system, as observed in simulations and DLS experiments. Another noteworthy observation was that systems involving PL 407 30 % and PL 407 15 %/PL 338 15 %, with hyaluronic acid, displayed increased mucoadhesive properties on mucin. This enhanced adhesion was possibly due to the role of hyaluronic acid as linking agent within mucin layers, by an independent manner of the poloxamer supramolecular structures. Conversely, the introduction of BVC or HA/BVC into the binary system reduced the force of detachment, likely due to the increased compactness of these hydrogels caused by the desolvation of the PO core. This highlighted the influence of all components and their chemical interactions on the relationship between structural organization and biological performance.

## CRediT authorship contribution statement

**Ana Ligia Scott:** Writing – original draft, Methodology, Investigation. **Daniele Ribeiro de Araujo:** Writing – original draft, Supervision, Funding acquisition, Conceptualization. **Fernando Carlos Giacomelli:** Investigation, Writing – original draft. **Anabella Patricia Rosso:** Investigation, Writing – original draft. **Anderson Ferreira Sepulveda:** Writing – review & editing, Writing – original draft, Investigation, Formal analysis, Conceptualization. **Jéssica Bassi da Silva:** Methodology, Investigation, Formal analysis. **Marcos Bruschi:** Writing – original draft, Supervision, Investigation. **Margareth Franco:** Methodology, Investigation. **Fabiano Yokaichiya:** Methodology, Investigation. **Giovana Tófoli:** Methodology, Investigation. **Cíntia Maria Cereda:** Methodology, Investigation.

## Declaration of Competing Interest

The authors declare the following financial interests/personal relationships which may be considered as potential competing interests: Daniele Ribeiro de Araujo reports financial support was provided by The Sao Paulo Research Foundation - FAPESP. Daniele Ribeiro de Araujo reports a relationship with National Council for Scientific and Technological Development that includes: funding grants. Anderson Ferreira Sepulveda has patent #Micellar Supramolecular Structure Software (MiSS). 2021. Software BR512021000746–8. Polymer analysis (POLYana). 2023. Software. BR512023001136–3 issued to Assignee. Nothing to declare If there are other authors, they declare that they have no known competing financial interests or personal relationships that could have appeared to influence the work reported in this paper.

## Data Availability

Data will be made available on request.

## Acknowledgements

The Sao Paulo Research Foundation - FAPESP (Grant 2014/14457-5, 2019/20303-4, 2021/12071-6, 2022/14668-2, 2023/13068-4), National Council for Scientific and Technological Development - CNPq (308819/2022-5). This study was also supported by The Coordenação de Aperfeiçoamento de Pessoal de Nível Superior—Brasil (CAPES)—Finance Code 001.

### *Authors contributions*

AFS and DRA contributed to the conceptualization, review, and manuscript writing. JBS and MLB performed the bioadhesive assays and wrote the manuscript. ALS contributed to molecular modelling and manuscript writing. MKKDF and FY contributed to investigation and analysis. GRT and CMSC performed cell viability assays and data analysis. FCG and APR conducted the simultaneous dynamic and static light scattering measurements and further data treatment.

### *Supplementary material*

Dynamic and static light scattering data. Correlation curves between bioadhesive tests and rheological analysis. Bonded interaction parameters for CG assays, simulated and experimental values of densities (kg/m$^3$), enthalpy $\boldsymbol{H}$ and radius of gyration $R_g$ of micelles.

## Appendix A. Supporting information

Supplementary data associated with this article can be found in the online version at doi:10.1016/j.colsurfa.2024.134527.

## References

[1] D.R. de Araujo, L.N.M. Ribeiro, E. de Paula, Lipid-based carriers for the delivery of local anesthetics, 2019, Expert Opin. Drug Deliv. 16 (2019) 701–714, https://doi.org/10.1080/17425247.2019.1629415.
[2] A.F. Sepulveda, R. Borges, J. Marchi, D.R. de Araujo, Biomedical applications of stimuli-responsive hydrogels (orgs), in: J.K. Patra, L.F. Fraceto, G. Das, E.V. R. Campos (Eds.), Green nanoparticles: synthesis and biomedical applications, Springer, 2020, https://doi.org/10.1007/978-3-030-39246-8_1.
[3] J.M. White, M.A. Calabrese, Impact of small molecule and reverse poloxamer addition on the micellization and gelation mechanisms of poloxamer hydrogels, Colloids Surf. A: Physicochem. Enginnering Asp. 638 (2022), https://doi.org/10.1016/j.colsurfa.2021.128246.
[4] M.H.M. Nascimento, M.K.K.D. Franco, F. Yokaichiya, E. de Paula, C.B. Lombello, D. R. de Araujo, Hyaluronic acid in Pluronic F-127/F-108 hydrogels for postoperative pain in arthroplasties: influence on physico-chemical properties and structural requirements for sustained drug-release, Int. J. Biol. Macromol. 111 (2018) 1245–1254, https://doi.org/10.1016/j.ijbiomac.2018.01.064.
[5] A.M. Bodratti, P. Alexandridis, Formulation of Poloxamers for drug delivery, J. Funct. Biomater. 9 (2018), https://doi.org/10.3390/jfb9010011.

[6] B. Schriky, A.A. Vigato, A.F. Sepulveda, I.P. Machado, D.R. de Araujo, Poloxamer-based nanogels as delivery systems: how structural requirements can drive their biological performance? Biophys. Rev. 15 (2023) 475–496, https://doi.org/10.1007/s12551-023-01093-2.

[7] G. Wanka, H. Hoffmann, W. Ulbrich, Macromolecules. Phase Diagrams and Aggregation Behavior of Poly(oxyethylene)-Poly(oxypropylene)-Poly(oxyethylene) Triblock Copolymers in Aqueous Solutions, Macromolecules (1994) 4145–4159, https://doi.org/10.1021/ma00093a016.

[8] P. Alexandridis, T.A. Hatton, Poly(ethylene oxide)-poly(propylene oxide)-poly (ethylene oxide) block copolymer surfactants in aqueous solutions and at interfaces: thermodynamics, structure, dynamics, and modeling, Colloids Surf. A: Physicochem. Eng. Asp. (1995) 1–46, https://doi.org/10.1016/0927-7757(94)03028-X.

[9] A.F. Sepulveda, M. Kumpgdee-Vollrath, M.K.K.D. Franco, F. Yokaichiya, D.R. de Araujo, Supramolecular structure organization and rheological properties modulate the performance of hyaluronic acid-loaded thermosensitive hydrogels as drug-delivery systems, J. Colloid. Interface Sci. B 630 (2023) 328–340, https://doi.org/10.1016/j.jcis.2022.10.064.

[10] L. Mayol, M. Biondi, F. Quaglia, S. Fusco, A. Borzacchiello, L. Ambrosio, M.I. La Rotonda, Injectable thermally responsive mucoadhesive gel for sustained protein delivery, Biomacromolecules 12 (2011) 28–33, https://doi.org/10.1021/bm1008958.

[11] S. Mansuri, P. Kesharwani, K. Jain, R.K. Tekade, N.K. Jain, Mucoadhesion: A promising approach in drug delivery system, 100, React. Funct. Polym. 100 (2016) 151–172, https://doi.org/10.1016/j.reactfunctpolym.2016.01.011.

[12] E. Giuliano, D. Paolino, M. Fresta, D. Cosco, Mucosal applications of Poloxamer407-based hydrogels: an overview, Pharmaceutics 10 (2018) 159, https://doi.org/10.3390/pharmaceutics10030159.

[13] G.P. Andrews, T.P. Laverty, D.S. Jones, Mucoadhesive polymeric platforms for controlled drug delivery, Eur. J. Pharm. Biopharm. 71 (2009) 505–518, https://doi.org/10.1016/j.ejpb.2008.09.028.

[14] R. Sankar, S.K. Jain, Development and characterization of gastroretentive sustained-release formulation by combination of swelling and mucoadhesive approach: a mechanistic study, Drug Des. Dev. Ther. 7 (2013) 1455–1469, https://doi.org/10.2147/DDDT.S52890.

[15] B.M. Boddupalli, Z.N. Mohammed, R.A. Nath, D. Banji, Mucoadhesive drug delivery: an overview, J. Adv. Pharm. Technol. Res. 1 (2010) 381–387, https://doi.org/10.4103/0110-5558.76436.

[16] M. Collado-González, Y.G. Espinosa, F.M. Goycoolea, Interaction between chitosan and mucin: fundamentals and applications, Biomimetics 4 (2019), https://doi.org/10.3390/biomimetics4020032.

[17] D. Song, D. Cahn, G.A. Duncan, Mucin biopolymers and their barrier function at airway surfaces, Langmuir 36 (2020) 12773–12783, https://doi.org/10.1021/acs.langmuir.0c02410.

[18] R.C. Boucher, Muco-obstructive lung diseases, N. Engl. J. Med. 380 (2019), https://doi.org/10.1056/NEJMra1813799.

[19] A.C.S. Akkari, J.Z.B. Papini, G.K. Garcia, M.K.K.D. Franco, L. Cavalcanti, A. Gasparini, M.I. Alkschbirs, F. Yokaichyia, E. de Paula, G.R. Tófoli, D.R. de Araujo, Poloxamer 407/188 binary thermosensitive hydrogels as delivery systems for infiltrative local anesthesia: physico-chemical characterization and pharmacological evaluation, Mater. Sci. Eng. C. 68 (2016) 299–307, https://doi.org/10.1016/j.msec.2016.05.088.

[20] D.A. Alves, D. Machado, A. Melo, R.F.C. Pereira, P. Severino, L.M. de Hollanda, D. R. de Araujo, M. Lancellotti, Preparation of thermosensitive gel for controlled release of levofloxacin and their application in the treatment of multidrug-resistant bacteria, Biomed. Res. Int. (2016), https://doi.org/10.1155/2016/9702129.

[21] M.H.M. Nascimento, F.N. Ambrosio, D.C. Ferraraz, H. Windisch-Neto, S. M. Querobino, M. Nascimento-Sales, M.A. Alberto-Silva, M.A. Christoffolete, M.K. K.D. Franco, B. Kent, F. Yokaichyia, C.B. Lombello, D.R. de Araujo, Sulforaphane-loaded hyaluronic acid-poloxamer hybrid hydrogel enhances cartilage protection in osteoarthritis models, Mater. Sci. Eng. C. 128 (2021), https://doi.org/10.1016/j.msec.2021.112345.

[22] L. Mayol, F. Quaglia, A. Borzacchiello, L. Ambrosio, M.I. La Rotonda, A novel poloxamers/hyaluronic acid in situ forming hydrogel for drug delivery: rheological, mucoadhesive and in vitro release properties, Eur. J. Pharm. Biopharm. 70 (2008) 199–206, https://doi.org/10.1016/j.ejpb.2008.04.025.

[23] A.F. Sepulveda, D.R. de Araujo, Bioadhesive behavior of Poloxamer/hyaluronic acid-based formulations analyzed by rheology method, *Sci. Talks* 1 10072 (2022), https://doi.org/10.1016/j.sctalk.2022.100072.

[24] I. Wood, J.M.R. Albano, P.L.O. Filho, V.M. Couto, M.A. de Farias, R.V. Portugal, E. de Paula, C.L.P. Oliveira, M. Pickholz, A sumatriptan coarse-grained model to explore diferente environments: interplay with experimental techniques. Eur. Biophys. J. 47 (2018) 561–571, https://doi.org/10.1007/s00249-018-1278-2.

[25] R. Kumar, Y.K. Lee, Y.S. Jho, Martini coarse-grained model of hyaluronic acid for the structural change of its gel in the presence of monovalent and divalent salts, Int. J. Mol. Sci. 21 (13) (2020), https://doi.org/10.3390/ijms21134602.

[26] S.J. Marrink, H.J. Risselada, S. Yefimov, D.P. Tieleman, A.H. de Vries, The MARTINI force field: coarse grained model for biomolecular simulations, J. Phys. Chem. B 111 (2007) 7812–7824, https://doi.org/10.1021/jp071097f.

[27] L. Martínez, R. Andrade, E.G. Birgin, J.M. Martínez, PACKMOL: a package for building initial configurations for molecular dynamics simulations, J. Comput. Chem. 30 (13) (2009) 2157–2164, https://doi.org/10.1002/jcc.21224.

[28] Hess et al. Gromacs user manual, version 4.5.4 (2010).

[29] S. Nawaz, P. Carbone, Coarse-graining poly(ethylene oxide)-poly(propylene oxide)-poly(ethylene oxide), J. Phys. Chem. B 118 (2014) 1648–1659, https://doi.org/10.1021/jp4092249.

[30] U. Adhikari, A. Goliaei, L. Tsereteli, M.L. Berkowitz, Properties of Poloxamer molecules and Poloxamer micelles dissolved in water and next to lipid bilayers: results from computer simulations, J. Phys. Chem. B 120 (2016) 5823–5830, https://doi.org/10.1021/acs.jpcb.5b11448.

[31] B. Raubenolt, G. Gyawali, W. Tang, K.S. Wong, S.W. Rick, Coarse-grained simulations of aqueous thermoresponsive polyethers, Polymers 10 (2018) 475, https://doi.org/10.3390/polym10050475.

[32] M. Abbaspour, M.N. Jorabchi, H. Akbarzadeh, A. Ebrahimnejad, Ikynvestigation of the thermal properties of phase change materials encapsulated in capped carbon nanotubes using molecular dynamics simulations. RSC Adv. 40 (2021) https://doi.org/10.1039/D1RA02033A.

[33] E. Yamamoto, T. Akimoto, A. Mitsutake, R. Metzler, Universal relation between relation between instantaneous diffusivity and radius of gyration of protein in aqueous solution, Phys. Rev. Lett. 126 (2021), https://doi.org/10.1103/PhysRevLett.126.128101.

[34] F. Eisenhaber, P. Lijnzaad, P. Argos, C. Sander, M. Scharf, The double cubic lattice method: efficient approaches to numerical integration of surface area and volume and to dot surface contouring of molecular assemblies, J. Comput. Chem. 16 (1995) 273–284, https://doi.org/10.1002/jcc.540160303.

[35] V. Lutsyk, P. Wolski, W. Plazinski, Extending the Martini 3 coarse-grained force field to carbohydrates, J. Chem. Theory Comput. 18 (2022) 5089–5107, https://doi.org/10.1021/acs.jctc.2c00553.

[36] S. Bhattacharjee, DLS and zeta potential – what they are and what they are not? J. Control. Release 235 (2016) 337–351, https://doi.org/10.1016/j.jconrel.2016.06.017.

[37] J. Stetefeld, S.A. McKenna, T.R. Patel, Dynamic light scattering: a practical guide and applications in biomedical sciences, Biophys. Rev. 8 (2016) 409–427, https://doi.org/10.1007/s12551-016-0218-6.

[38] M.L. Bruschi, D.S. Jones, H. Panzeri, M.P.D. Gremião, O. de Freitas, E.H.G. Lara, Semisolid Systems Containing Propolis for the Treatment of Periodontal Disease: In Vitro Realease Kinetics, Syringeability, Rheological, Textural and Mucoadhesive Properties, J. Pharm. Sci. 99 (2007) 4215–4227, https://doi.org/10.1002/jps.20843.

[39] J. Bassi da Silva, S.B.S. Ferreira, O. de Freitas, M.L. Bruschi, A critical review about methodologies for the analysis of mucoadhesive properties of drug delivery systems, Drug Dev. Ind. Pharm. 9045 (2017) 1–67, https://doi.org/10.1080/03639045.2017.1294600.

[40] J. Bassi da Silva, S.B.S. Ferreira, A.V. Reis, M.T. Cook, M.L. Bruschi, Assessing mucoadhesion in Polymer gels: the effect of method type and instrument variables, Polymers 10 (2018), https://doi.org/10.3390/polym10030254.

[41] M. Bathe, G.C. Rutledge, A.J. Grodzinsky, B. Tidor, A coarse-grained molecular model for glycosaminoglycans: application to chondroitin, chondroitin sulfate, and hyaluronic acid, Biophys. J. 88 (2005) 3870–3887, https://doi.org/10.1529/biophysj.104.058800.

[42] L. Tsereteli, A. Grafmüller, An acccurate coarse-grained model for chitosan polysaccharides in aqueous solution. PLoS One 12 (7) (2017) https://doi.org/10.1371/journal.pone.0180938.

[43] W. Wu, Z. Zou, S. Yang, Q. Wu, W. Li, Q. Ding, Z. Guan, W. Zhu, Coarse-Grained Molecular Dynamic and Experimental Studies on Self-Assembly Behavior of Nonionic F127/HS15 Mixed Micellar Systems, Langmuir 36 (2020) 2082–2092, https://doi.org/10.1021/acs.langmuir.9b03936.

[44] A. Kantardjiev, P.M. Ivanov, Entropy rules: molecular dynamics simulations of model oligomers for thermoresponsive polymers, Entropy 22 (2020), https://doi.org/10.3390/e22101187.

[45] A. Oshiro, D.C. da Silva, J.C. de Mello, V.W.R. de Moraes, L.P. Cavalcanti, M.K.K. D. Franco, M.I. Alkschibirs, L.F. Fraceto, F. Yokaichyia, T. Rodrigues, D.R. de Araujo, Pluronics F-127/L-81 binary hydrogels as drug-delivery systems: influence of physicochemical aspects on release kinetics and cytotoxicity, Langmuir 30 (2014) 13689–13698, https://doi.org/10.1021/la503021c.

[46] N.I. Ercan, P. Stroeve, J.W. Tringe, R. Faller, Understanding the interaction of Pluronic L61 and L64 with a DOPC lipid bilayer: an atomistic molecular dynamics study, Langmuir 32 (2016) 10026–10033, https://doi.org/10.1021/acs.langmuir.6b02360.

[47] I.M. Hansen, M.F. Ebbesen, L. Kaspersen, T. Thomsen, K. Bienk, Y. Cai, B.M. Malle, K.A. Howard, Hyaluronic acid molecular weight-dependent modulation of mucin nanostructure for potential mucosal therapeutic applications, Mol. Pharm. 14 (2017) 2359–2367, https://doi.org/10.1021/acs.molpharmaceut.7b00236.

[48] R.V. Pai, J.D. Monpara, P.R. Vavia, Exploring molecular dynamics simulation to predict binding with ocular mucin: An in silico approach for screening mucoadhesive materials for ocular retentive delivery systems, J. Control. Release 309 (2019) 190–202, https://doi.org/10.1016/j.jconrel.2019.07.037.

[49] X. Gao, Y. Xiong, H. Chen, X. Gao, J. Dai, Y. Zhang, W. Zou, Y. Gao, Z. Jiang, B. Han, Mucus adhesion vs. mucus penetration? Screening nanomaterials for nasal inhalation by MD simulation, J. Control. Release 353 (2023) 366–379, https://doi.org/10.1016/j.jconrel.2022.11.051.

[50] J. Armstrong, B. Chowdhry, J. Mitchell, A. Beezer, S. Leharne, Effect of Cosolvents and Cosolutes upon Aggregation Transitions in Aqueous Solutions of the Poloxamer F87 (Poloxamer P237): A High Sensitivity Differential Scanning Calorimetry Study, J. Phys. Chem. 100 (1996) 1738–1745, https://doi.org/10.1021/jp951390s.

[51] I. Wood, M.F. Martini, J.M.R. Albano, M.L. Cuestas, V.L. Mathet, M. Pickholz, Coarse grained study of pluronic F127: Comparison with shorter co-polymers in its interaction with lipid bilayers and self-aggregation in water, J. Mol. Struct. 1109 (2016) 106–113, https://doi.org/10.1016/j.molstruc.2015.12.073.

[52] F.C. Carvalho, G. Calixto, I.N. Hatakeyama, G.M. Luz, M.P.D. Gremião, M. Chorilli, Rheological, mechanical, and bioadhesive behavior of hydrogels to optimize skin

delivery systems, Drug Dev. Ind. Pharm. (2012), https://doi.org/10.3109/03639045.2012.734510.

[53] K.C.F. Mariano, J.Z.B. Papini, N.C. de Faria, D.N.C. Heluany, A.L.L. Botega, C.M. S. Cereda, E. de Paula, G.R. Tófoli, D.R. de Araujo, Ropivacaine-loaded Poloxamer binary hydrogels for prolonged regional anesthesia: structural aspects, biocompatibility, and pharmacological evaluation, Biomed. Res. Int. (2021), https://doi.org/10.1155/2021/7300098.

[54] A.C.M. dos Santos, A.C.S. Akkari, I.R. Ferreira, C.R. Maruyama, M. Pascoli, V. A. Guilherme, E. de Paula, L.F. Fraceto, R. de Lima, P.S. Melo, D.R. de Araujo, Poloxamer-based binary hydrogels for delivering tramadol hydrochloride: sol-gel transition studies, dissolution-release kinetics, in vitro toxicity, and pharmacological evaluation, *Int. J. Nanomed.* 10 (2015) 2391–2401, https://doi.org/10.2147/IJN.S72337.